Mechanical modeling of carbonic anhydrase motion in simple channels

Y. B. Yi[a] and C. S. Lengsfeld
Department of Engineering, University of Denver, Denver, Colorado 80208

(Received 11 January 2006; accepted 14 April 2006; published online 7 July 2006)

The difference in potential energy generated by molecular confinement arising from molecular length has a potential application to separation technology. However, the design and optimization of an integrated microfluidic device to detect and separate chemically similar molecules will require computational techniques capable of predicting the energy storage (or release) associated with conformational change. To this end we developed midlevel modeling approach for the prediction of macromolecular motion in a confinement channel using finite element analysis and stochastic methods. As a proof of concept, we investigated the mechanical behavior of a carbonic anhydrase molecule where the molecule was modeled as a beam network constructed by the backbone carbon atoms. Each pair of the adjacent atoms form an elastic beam that bears both axial and shear stresses. The molecular conformation and associated dynamic behavior of the reconstructed molecule were investigated via two protocols: (1) compression of the molecule under a pair of parallel plates; and (2) propagation of the molecule through a shrinking channel. The probabilistic simulation results along with the characteristic velocity profiles demonstrate the capability of this approach to capture physically relevant behavior. © *2006 American Institute of Physics*. [DOI: 10.1063/1.2208561]

I. INTRODUCTION

Conventional DNA purification techniques have been adapted from principles governing protein purification, but the copurification of *E. coli* chromosomal DNA and RNA presents a unique challenge due to their similar physical and chemical properties to those of the product (i.e., plasmid DNA). Cell lysis, differential precipitation, enzymatic digestion, column chromatography, desalting, buffer exchange, and sterile filtration represent the typical processing steps that result in the fragmentation of long, linear forms of DNA. As a result, contemporary plasmid purification protocols sacrifice approximately 30%–50% of the therapeutic plasmid in an attempt to minimize genomic DNA contamination. Innovative real-time solutions to the monitoring and control of contamination problems during bioprocessing could have an enormous impact on the economics of gene therapy as well as other macromolecular processing strategies.

Exploiting molecular propulsion mechanisms for a separation technology is a recent concept. Some work already exists in the area of utilizing micron or submicron fluidic devices to enhance DNA separation techniques. Most of these techniques utilize electric fields or electro-osmotic flow[1] to induce movement in these macromolecules but rely on differences in molecular potential energy to induce separation. Electric field induced diffusion through cylindrical or rectangular obstacles set at an angle of 45° to the field has demonstrated that small molecules move faster than large ones, making continuous sorting possible.[2,3] Switching the electric field in 10 s intervals to DNA within similar configurations has shown enhanced separation rates by slowing the larger molecules even more.[4,5] Instead of rectangular post arrays, Han and Craighead[6] demonstrated that changes in macromolecular confirmation by altering the channel dimension from thick to thin can create entropic traps that collect a particular size range. These confinement channels separate DNA fragments of different sizes utilizing the concept that as channel size approaches the molecular scale or smaller, the channel walls prohibit some molecular conformations.[7–9] These limitations result in excess free energy (or an entropy gradient) which may impart a measurable force. For example, Turner *et al.*[7] reported forces on the order of femtonewtons that is proportional to molecular length. Therefore matrices could be designed such that only a specific length scale will have the necessary inherent force to move through the system.

This work builds off these observations to develop an efficient computational technique that could be utilized to design and optimize microfluidic separation devices. The traditional approach to modeling macromolecular behavior has been molecular dynamic simulations.[10–12] However these techniques are computationally time intensive and therefore limited to relatively small molecular lengths. Essentially molecular dynamic simulations compute the attraction and repulsion forces between atoms as a function of distance. We propose to eliminate this complex and time consuming step by simulating the interaction with an elastic beam. Additionally, because the molecules of interest (i.e., DNA) are large but fundamentally composed of subunits (e.g., nucleotide), the molecule can be treated as small units bonded into long chains as done previously by Rzehak *et al.*[13] and Hur and Shaqfeh.[14] Again this kind of chain network can be modeled as an equivalent beam system possessing either elastic or hyperelastic material properties.[15–17]

The work presented here uses a model molecule that is considerably smaller than DNA, but is well characterized. The carbonic anhydrase molecule was computationally reconstructed by bonding its backbone carbon atoms to demonstrate the ability of this technique to capture the impact of

[a]Author to whom correspondence should be addressed; electronic mail: yyi2@du.edu

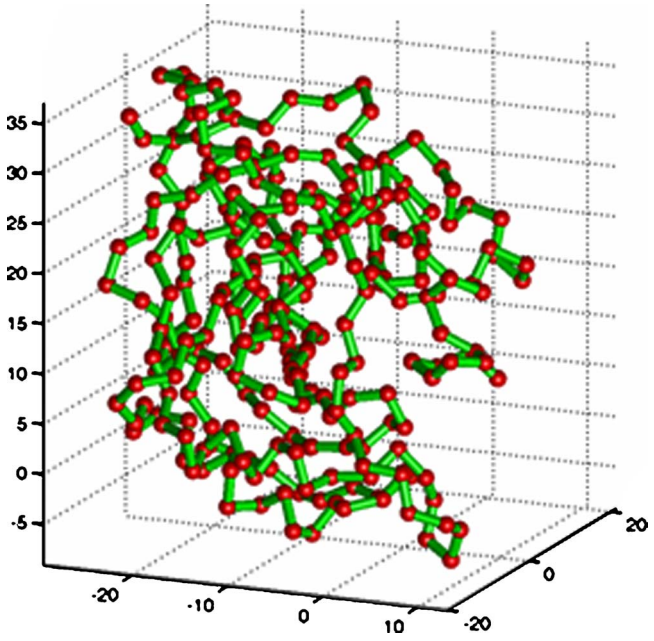

FIG. 1. Carbonic anhydrase (CA) molecule reconstructed as an elastic beam network by connecting carbon atoms along the backbone. The axes represent the dimensions in the x, y, and z directions (unit: Å).

conformation on stored energy and relate this to the well understood phenomena of molecular motion through a converging nozzle throat.

II. METHOD

A. Computational reconstruction of macromolecules

As a proof of concept, we characterized and computationally reconstructed a carbonic anhydrase (CA) molecule, which possesses a relatively simple structure compared to those of DNA molecules. As an enzyme that catalyzes the hydration of carbon dioxide and the dehydration of bicarbonate, CA has been found in all animals and photosynthesizing organisms.[18] In this study we modeled a CA molecule (Carbonic Anhydrase II Mutant E117Q, Apo Form[19]) as an elastic beam network connected by the carbon atoms along its backbone, with each pair of adjacent carbon atoms forming a Timoshenko beam that bears both axial and shear stresses, as shown in Fig. 1. The spatial coordinates of the atoms were extracted from the three-dimensional (3D) macromolecular structure database available in the Protein Data Bank (RCSB PDB).[20] The total number of carbon atoms is 257, and the corresponding number of elastic beams is 256. The beams are rigidly bonded at the intersection points where the carbon atoms reside.

B. Compression with parallel plates

To study the mechanical behavior of CA molecule in a confinement geometry, we first studied molecular deformation under static conditions to see if conformation change indeed translated into stored energy and to ensure that the code naturally converges to a minimum volume or maximum deformation—specifically, the molecular beam network was gradually deformed under the compression of a pair of rigid planes subject to uniform downward displacement. In order to isolate the impact of molecular compression on motion and conformation, a frictionless contact condition was incorporated by using a set of gap elements between the corresponding nodes on the beams and the rigid planes. Gap elements are special types of structural elements used to model the interface between portions of a structure where contact or separation can occur. Gap elements support compression loading, but they cannot support axial tension. Therefore, an iterative solution procedure was used to solve the relevant contact problem. Gaps that were in contact and transmitted axial compression between the end joints were identified as closed. All other joints were identified as open. Iteration continued until a stable set of closed gaps were found that were in equilibrium with applied loads.

Briefly, the formulation of the contact problem was such that the nodal contact scheme was used and the penetration of the corresponding nodes was examined during each time step of numerical iteration. The compression was assumed to be very slow, and thus dynamic instabilities of the system (e.g., internal wave propagations) were negligible and not investigated. For the boundary conditions, the structure was constrained at one end of the beam chain but free at the other end; the rigid planes were constrained along all the directions except the direction of compression.

C. Deformation in nonuniform channels

The second step in evaluating this approach was to observe the dynamic or transient behavior of the molecule through a confined channel. Again we will seek to obtain volume limits, which in this geometry will lead to orifice plugging and capture physically relevant behavior by assessing the impact of wall friction factors on molecular behavior.

The material properties of beams were not changed from those in the initial parallel plate simulation; however, different boundary and initial conditions were applied: walls were no longer parallel, all the degrees of freedom on the channel were constrained during the simulation, and the molecule was assigned with an initial propagation velocity. The contact condition between the walls and the molecule was frictionless unless otherwise noted, in order to highlight behavior changes arising from bond or beam compression. The numerical approach prescribed a coefficient of friction between the element-based surface constructed on the rigid plate elements and node-based surfaces constructed on the beam elements. The commercial software package ABAQUS/EXPLICIT was used to perform the transient dynamic analysis.

Even though the dynamic instability or kinetic wave propagation inside the solid material was beyond the scope of this project, and a quasistatic solution could be utilized to minimize the inertia effects caused by contact, this approach remained computationally cumbersome at long time scales (e.g., requiring an excessive number of small time increments). We found that the speed of the analysis could be enhanced substantially without severely degrading the quality of the quasistatic solution, by choosing appropriate simulation parameters such as those listed in Table I. Since the flows under investigation have small Reynolds numbers, the

TABLE I. Simulation parameters in finite element analysis.

Beam section	Elastic modulus	Density	Initial velocity	Increment number	Simulation time
0.01 Å (diameter)	1.0×10^{12} Pa	100 kg/m^3	150 Å/s	~200 000	1.0 s

inertial term (i.e., density) does not impact the dynamic behavior. Therefore the value of density was based on the model performance in favor of faster speed in solution convergence. As one would predict, the converged result remained unchanged from the full quasistatic solution under a wide range of loading speed (i.e., initial propagation speed), except when the loading speed was increased to a point at which inertial effects dominated. As the inertial term becomes dominant, the solution localizes and diverges from the quasistatic solution. These conditions occur, for example, when the molecule moves at a high speed $\sim1.0\times10^4$ Å/s, and as a result the beams in the front undergo severe deformation before their transferring the load to the beams in the rear. In general, quasistatic solutions for molecular deformation are not sensitive to those simulation parameters such as density and modulus. However, in the cases where we are concerned with the development of local stresses inside the molecule, experimentally measured parameters should be used in all the simulations.

D. Incorporation of uncertainties in simulation

Molecular behaviors are stochastic in a confined geometry due to three factors: (1) the probabilistic orientation and spatial location of a molecule in a microfluidic device; (2) molecular conformation; and (3) internal entropy effect on internal structure or bond length. The last factor is presumably not as dominant as the first two. The difficulties associated with the geometric variation in molecular conformation will be discussed in later studies specifically interested in the impact of structurally limited degrees of freedom.

This study therefore only considers the impact of randomness induced by the geometric asymmetry of the molecular surface, namely, the uncertainties in the spatial orientation of molecule. The numerical treatments on randomness of an asymmetric body were well addressed by Yi *et al.*,[21] for modeling triaxial ellipsoidal particles in Li-ion batteries, and Yi *et al.*,[22] for modeling intracellular calcium transport, and were thus directly applied to this study. Because this molecular orientation is difficult to measure or monitor in experiments, it has been treated as a probabilistic variable. The mathematical representation of this variable was realized by applying a rotation matrix on the spatial displacements of the nodes, based on the Monte Carlo simulation method for asymmetric geometries introduced by Yi and Sastry.[23,24] In general, we have

$$\begin{bmatrix} u-x_0 \\ v-y_0 \\ w-z_0 \end{bmatrix} = \Omega \begin{bmatrix} x-x_0 \\ y-y_0 \\ z-z_0 \end{bmatrix}, \tag{1}$$

in which x_0, y_0, and z_0 represent the centroidal positions of molecule; x, y, z are the original nodal positions; u, v and w are the nodal positions after rotation; and Ω is the rotation matrix. Mathematically, in $\Re^3$, rotations about the x, y, and z axes require operations,

$$\Omega_x(\alpha) = \begin{bmatrix} 1 & 0 & 0 \\ 0 & \cos\alpha & \sin\alpha \\ 0 & -\sin\alpha & \cos\alpha \end{bmatrix},$$

$$\Omega_y(\beta) = \begin{bmatrix} \cos\beta & 0 & -\sin\beta \\ 0 & 1 & 0 \\ \sin\beta & 0 & \cos\beta \end{bmatrix},$$

$$\Omega_z(\gamma) = \begin{bmatrix} \cos\gamma & \sin\gamma & 0 \\ -\sin\gamma & \cos\gamma & 0 \\ 0 & 0 & 1 \end{bmatrix}. \tag{2}$$

Because any arbitrary rotation can be decomposed into rotations about each of the three axes, we can write a three by three rotation matrix as

$$\Omega = \Omega_x(\alpha)\Omega_y(\beta)\Omega_z(\gamma). \tag{3}$$

The orientation of the triaxes of a three-dimensional Poissonian system can be described in an Euler system, by the azimuthal/rotational angles having uniform probability densities and the polar angle having a probability density function biased towards the equator. This issue has extensively been discussed in the authors' previous publications.[23,25] By incorporating this factor, finite element simulations with randomized orientation parameters were performed and the statistical results were computed.

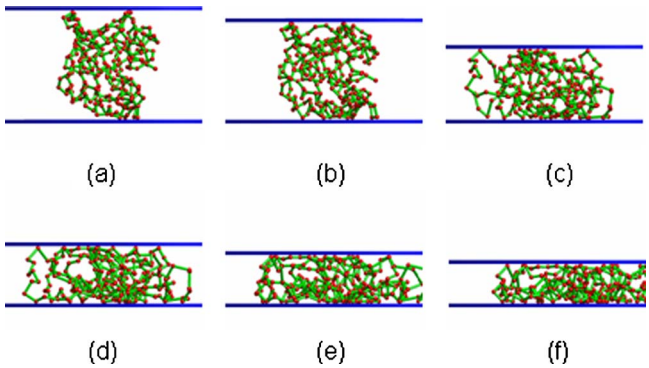

FIG. 2. Sequential images showing the deformation of a CA molecule under the confinement of two rigid plates under (a) 0% deformation; (b) 15% deformation; (c) 30% deformation; (d) 50% deformation; (e) 70% deformation; (f) and 80%. Deformation ratio is defined as the plate displacement divided by the maximum allowable value.

III. RESULTS

A. Deformation under parallel plates

The sequential images in Fig. 2 show the deformation of a CA molecule under the compression of two rigid plates with gradually increased deformation ratios. Notice that even in a simulation where motion in a direction was not anticipated, the confinement generated a lateral motion to the right. Moreover, the simulation results revealed that the process is highly stochastic and some portions of the beams

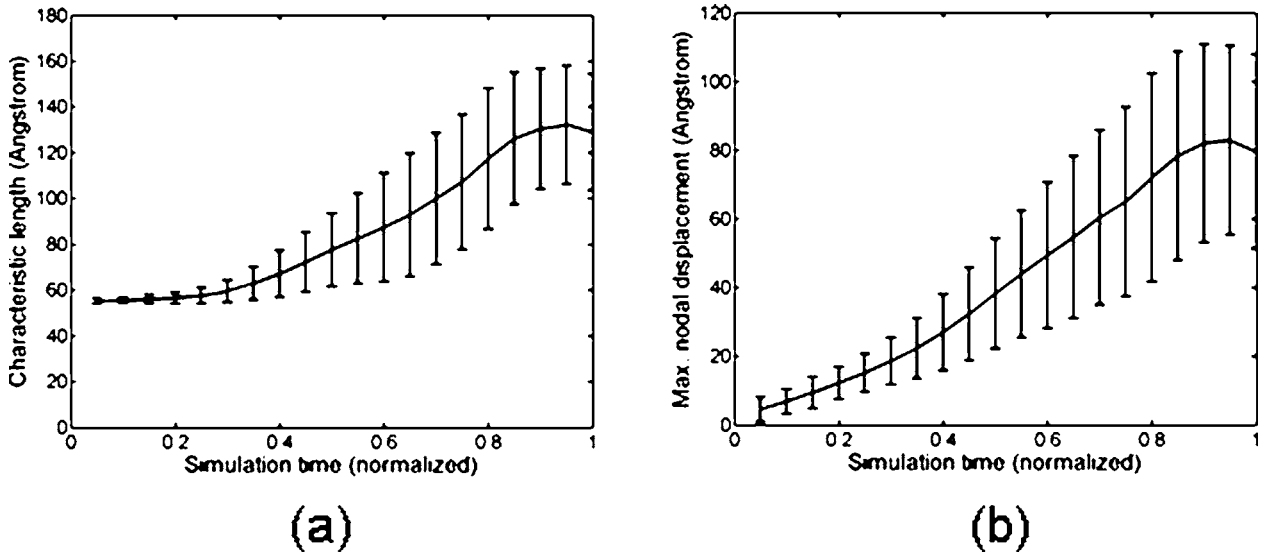

FIG. 3. (a) Characteristic length of CA molecule as a function of normalized simulation time; (b) maximum nodal displacement vs normalized simulation time. The standard deviations of the results are shown as error bars. Unit shown on the vertical axes is Å. In both (a) and (b) fifty simulations were run to obtain the statistical results.

could extend outside of the original structure (Fig. 2), causing significant changes in the characteristic molecular length, as shown in Fig. 3(a). That is to say, the characteristic length of molecule, defined here as the largest possible distance between any pair of the nodes inside the molecule, changed during compression. For example, under 60% deformation ratio (that is, when the distance traveled by the plate divided by its maximum allowed value was 0.6), the mean characteristic length (90 Å) has increased by 50% of the original diameter (60 Å), while its variation (2× standard deviation) is as much as 100% of its original diameter, as shown in Fig. 3(a). During the later stages of compression, the curve of mean characteristic length has arrived at a plateau (130 Å), implying that the structure is nearly self-locked and further change in its characteristic length is no longer possible. This resembles an upright-positioned coiled spring and the compression would not induce any changes in its transverse length. Thus the change in molecular conformation is not a simple function of the distance traveled by the rigid plate as would be expected in an idealized elastic body.

The maximum nodal displacement is also substantial, with an averaged plateau value (80 Å) larger than the original molecule diameter [Fig. 3(b)]. The large nodal displacements are suspected to have correlations with the entropy gradient induced by the confinement. Meanwhile, the geometric center of the molecule does not move significantly, only about 30 Å with the standard deviation of around 20 Å. This is not surprising, because the movement of the mass center is solely activated by the reactions exerted at the constrained node on the long chain.

The results above have strongly shown that the geometric asymmetry of CA molecule results in significant variation in the deformed conformation, which alters the potential energies stored in the molecule. When such a molecule travels through microfluidic channels, the shear forces caused by the local confinement of channels will convert some of the molecules' kinetic energy into potential energy or *vice versa* and thus change their translational and angular velocities. The amount of change in velocities, however, is probabilistic due to the large variation in the stored potential energy.

B. Deformation under nonuniform channel

Parametric studies with nonuniform channels were performed on four variables: (1) the randomness in the molecular orientation; (2) the diameter of the channel throat (or orifice); (3) angle of inclination of the plates leading to the orifice; and (4) the coefficient of Coulomb friction on the contact surfaces. In varying the orifice diameter, we maintained the angle of channel inclination to be unchanged; in varying the inclination angle, however, the orifice diameter at the exit maintained unchanged, as shown in Fig. 4. If the orifice angle were sufficiently small, the molecule would have to be predeformed before entering the orifice, which would change the model's initial condition and make it difficult to compare the results obtained from different inclination angles. In view of this, the minimum inclination angle was set to 20° to avoid possible interference between the molecule and the channel wall at the beginning of the process.

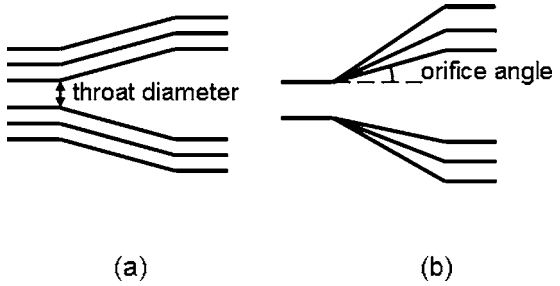

FIG. 4. Schematic of the channel geometry for parametric analysis: (a) different throat diameters under the same orifice angle; (b) different orifice angles under the same throat diameter.

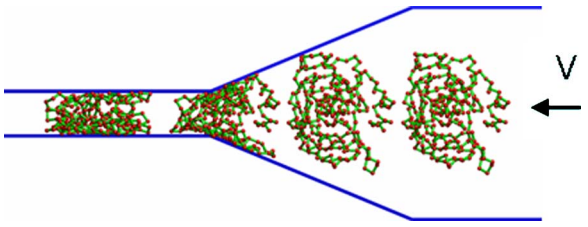

FIG. 5. Finite element simulation showing the deformation of a CA molecule when it travels through a shrinking channel.

The simulation results were plotted in the form of velocity profiles in the time domain. It has been found that a typical velocity profile consists of three distinct phases: The first phase is the period between the beginning of each simulation and the time when the molecule makes the first contact with the plates. In this phase, the molecule moves as a whole at constant velocity and there is no rotational or vibrating motion in the structure since no external loading is applied. The second phase is the period when the molecule is in contact with the plates. During this phase, the normal forces and the friction forces are directed opposite to the molecular movement and thus reduce the overall velocity. The third and the last phase is defined here as the period after the molecule completely exits the orifice of the channel and the molecule-channel contact is lost. After the exit, the potential energy stored in the compressed beam system is released, which then leads to structural vibration and rotation. Please notice that the release of the stored potential energy will not cause an increase of the bulk propagation velocity (i.e., mean velocity of all the beams in the structure). In the case of frictionless contact, after the molecule loses contact with the channel, the external forces would no longer be present and thus the mean velocity would remain constant.

A sequence of static images is presented in Fig. 5, showing the change of profile in the molecule's geometry when it squeezed through the channel. Notice that the molecule tended to return to its original shape after it exited the channel throat. However, the downstream part of the channel has a diameter smaller than that of the molecule and as a result, the molecule remained under constraints. Detailed study on the images revealed that not only the translational velocity of the beam structure but also its angular velocities were altered due to the geometric heterogeneity in both tangential (in-plane) and transversal (out-of-plane) directions.

By running the simulation with randomized orientation angles of molecule, it has been found that the variation in the velocity is usually non-negligible. For example, when the orifice angle is 25° and the coefficient of friction is zero, the velocity shows a mild variation with standard deviation of about 2% of the mean value, as shown in Fig. 6(a); when the orifice has a larger inclination angle or the coefficient of friction becomes nonzero, standard deviations as high as 10%–20% of the mean velocity were observed in the simulations. This again confirms that the process is highly probabilistic. Since acceleration is the time derivative of velocity, the acceleration profile in Fig. 6(b) exhibits even stronger randomness with standard deviation of nearly 50% of the maximal mean acceleration. In view of these characteristic profiles, the consideration of statistics is essential in practical applications.

Apparently, when the orifice angle increases, the velocity of molecule will further decrease. Figure 7 shows the result of mean propagation velocity as a function of simulation time under different orifice angles. The kinetic friction coefficient has a zero value in all the cases to highlight effects resulting from bond or beam deflection rather than complicated by other sources of kinetic energy loss. A later figure will compare molecular behaviors over a range of friction factors that are relevant to microfluidics (e.g., Bhushan and Burton[26]). When the angle is sufficiently small, the molecule will eventually come to stop and then bounce back. This bouncing back behavior is very interesting and may have potential applications; however, in the current study we are

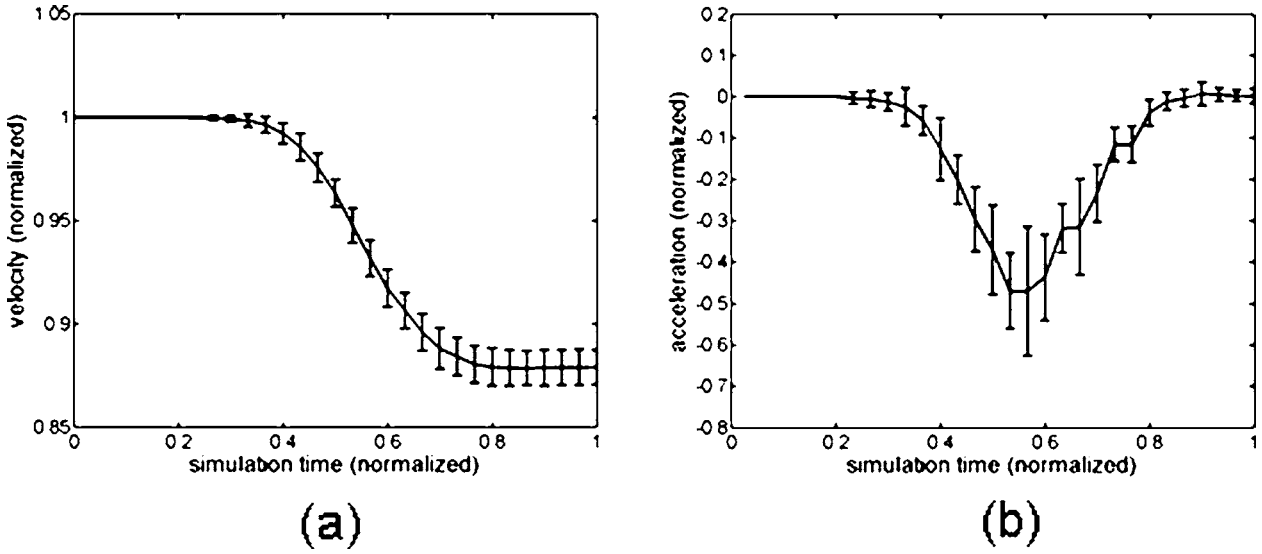

FIG. 6. (a) Translational velocity as a function of time when a CA molecule travels through a shrinking channel. The randomness in the molecular orientation is considered. The velocity is normalized by its initial value. (b) Acceleration as a function of time. The acceleration is normalized by the initial velocity divided by the simulation time. The error bars show the standard deviations. Ten simulations were run to obtain the statistical results.

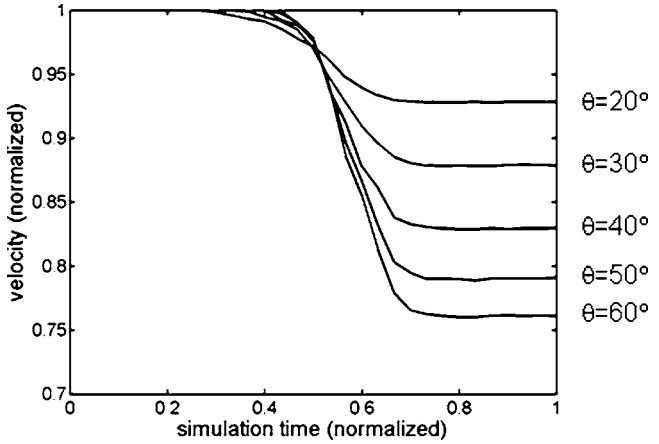

FIG. 7. Effect of orifice angle on the translational velocity when a CA molecule travels through a shrinking channel. The velocity is normalized by its initial value.

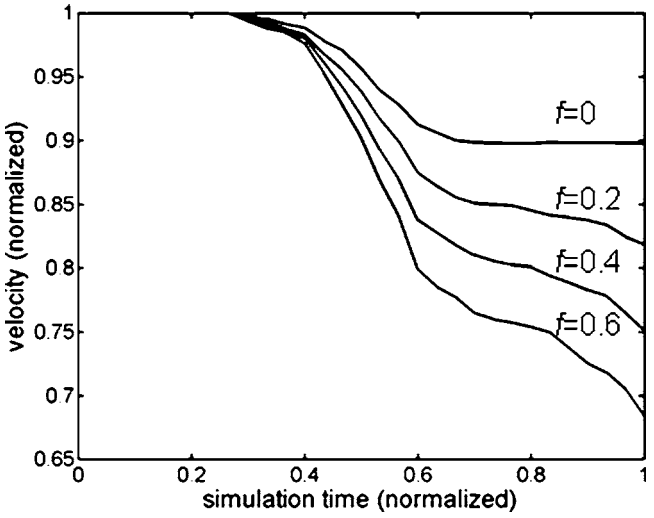

FIG. 9. Effect of Coulomb friction on the translational velocity when a CA molecule travels through a shrinking channel. The velocity is normalized by its initial value.

not attempting to explore the details of this phenomenon thus limiting ourselves to the forward motion of molecule.

When the throat diameter increases, the velocity of molecule will also increase, which is consistent with the conservation of energy. Figure 8 shows the result of mean propagation velocity as a function of simulation time under different throat diameters. Again, the kinetic friction coefficient was set to zero in all the cases. When the throat diameter was larger than the molecular size, apparently, the molecule experienced no interaction with the channel walls and thus no reductions or variations in velocity were observed.

Coulomb friction causes energy dissipation and thus reduces propagation velocity. Figure 9 displays the velocity profile under different values of friction coefficient from zero to 0.6. This range is consistent with those measured in microfluidic systems by Bhushan and Burton,[26] who found coefficients of friction values of 0.2 in poly(methyl methacrylate) or PMMA channels, 0.4 in single-crystal silicon substrates, and 0.6 in polydimethylsiloxane or PDMS channels. All the other parameters are the same and the channel angle is fixed to be 25°. It is important to know that the reduction in velocity persists even when the contact is frictionless. In frictionless contact, there would be no energy dissipation and the linear kinetic energy lost in the process would be converted into other types of energy in the form of rigid body rotation or structural vibration. On each of the curves in Fig. 9, a single simulation was performed with the same molecular orientation angle. Statistical averages would have revealed similar trends of results if multiple simulations had been performed. It turns out that under the parameters investigated, the translational velocity will be reduced as much as 30% when the coefficient of friction is 0.6.

The phenomena associated with velocity loss of molecules in small channels can be utilized to separate molecules of different types because the dynamic responses of different molecules will vary depending on molecular size and shape. For example, a molecule of larger minimum volume or a molecule possessing irregular surface shape will experience larger losses in translational velocity compared to smaller and more spherical molecules. Different velocity profiles obtained from simulations can thus be directly used in the design of microchannels for the purpose of molecule separation, as mentioned previously.

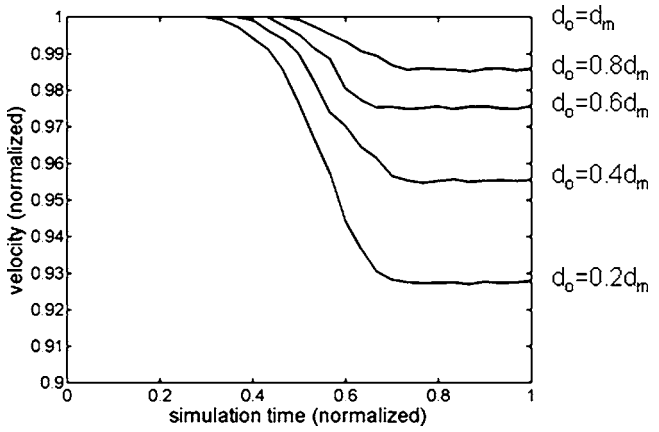

FIG. 8. Effect of channel throat diameter on the translational velocity when a CA molecule travels through a shrinking channel. The velocity is normalized by its initial value. d_o is throat diameter; d_m is the original molecular length in the z direction (perpendicular to translational velocity).

IV. CONCLUSION

A methodology has been developed for modeling macromolecular motions in confinement channels using finite element analysis and stochastic approach. Conformational changes of a representative molecule led both to the storage and release of potential energy. Most importantly the approach correctly predicted the retardation of the molecule through an orifice smaller than the minimum volume. To our surprise the simulations revealed an ability for locomotion due to stored energy, but the direction and velocity were stochastic depending on initial molecular orientation within the channel. Future studies need to focus on incorporating the impact of fluid solid interactions as well as bond limiting degrees of freedom.

[1]L. R. Huang, J. O. Tegenfeldt, and J. Kraeft, Nat. Biotechnol. **20**, 1048 (2002).
[2]C. F. Chou, O. Bakajin, S. W. P. Turner, T. A. J. Duke, S. S. Chan, E. C. Cox, H. G. Craighead, and R. H. Austin, Proc. Natl. Acad. Sci. U.S.A. **96**, 13762 (1999).
[3]N. Kaji, Y. Tezuka, Y. Takamura, M. Ueda, T. Nishimoto, H. Nakanishi, Y. Horiike, and Y. Baba, Anal. Chem. **76**, 15 (2004).
[4]O. Bakajin, T. A. J. Duke, J. Tegenfeldt, C. F. Chou, S. S. Chan, R. H. Austin, and E. C. Cox, Anal. Chem. **73**, 6053 (2001).
[5]K. D. Cole and C. M. Tellez, Biotechnol. Prog. **18**, 82 (2002).
[6]J. Han and H. G. Craighead, Science **288**, 1026 (2000).
[7]S. W. P. Turner, M. Cabodi, and H. G. Craighead, Phys. Rev. Lett. **88**, 128103 (2002).
[8]M. Cabodi, S. W. P. Turner, and H. G. Craighead, Anal. Chem. **74**, 5169 (2002).
[9]M. Foquet, J. Korlach, W. Zipfel, W. W. Webb, and H. G. Craghead, Anal. Chem. **74**, 1415 (2002).
[10]L. Mirny and E. Shakhnovich, Annu. Rev. Biophys. Biomol. Struct. **30**, 361 (2001).
[11]J. E. Shea and C. L. Brooks, Annu. Rev. Phys. Chem. **52**, 499 (2001).
[12]J. N. Onuchic, Z. Lutheyschulten, and P. G. Wolynes, Annu. Rev. Phys. Chem. **48**, 545 (1997).
[13]R. Rzehak, W. Kromen, T. Kawakatsu, and W. Zimmerman, Eur. Phys. J. E **2**, 3 (2000).
[14]J. S. Hur and E. S. G. Shaqfeh, J. Rheol. **45**, 421 (2000).
[15]L. Berhan, Y. B. Yi, A. M. Sastry, E. Munoz, M. Selvidge, and R. Baughman, J. Appl. Phys. **95**, 4335 (2004).
[16]L. Berhan, Y. B. Yi, and A. M. Sastry, J. Appl. Phys. **95**, 5027 (2004).
[17]Y. B. Yi, L. Berhan, and A. M. Sastry, J. Appl. Phys. **96**, 1318 (2004).
[18]M. J. Loferer, C. S. Tautermann, H. H. Loeffler, and K. R. Liedl, J. Am. Chem. Soc. **125**, 8921 (2003).
[19]C. C. Huang, C. A. Lesburg, L. L. Kiefer, C. A. Fierke, and D. W. Christianson, Biochemistry **35**, 3439 (1996).
[20]RCSB Protein Data Bank, http://www.rcsb.org/pdb/.
[21]Y. B. Yi, C. W. Wang, and A. M. Sastry, ASME J. Eng. Mater. Technol. **128**, 73 (2006).
[22]Y. B. Yi, H. Wang, A. M. Sastry, and C. M. Lastoskie, Phys. Rev. E **72**, 021913 (2005).
[23]Y. B. Yi and A. M. Sastry, Proc. R. Soc. London, Ser. A **460**, 2353 (2004).
[24]Y. B. Yi and A. M. Sastry, J. Comput. Phys. (submitted).
[25]Y. B. Yi, C. W. Wang, and A. M. Sastry, J. Electrochem. Soc. **151**, A1292 (2004).
[26]B. Bhushan and Z. Burton, Nanotechnology **16**, 467 (2005).